environments

Article

Phytoremediation Potential of Native Species in Arid Soils Impacted by Gold Mining

Belén Heredia [1,2,3,*], Brian Jonathan Young [4,5], Pablo Pacheco [6], Hernán P. Burrieza [7], María Inés Mercado [8] and Gonzalo Roqueiro [2,3]

1 Consejo Nacional de Investigación Científica y Técnica (CONICET-CCT Mendoza), Av. Ruiz Leal s/n—Parque Gral. San Martín, Mendoza M5500BWC, Argentina
2 Estación Experimental Agropecuaria San Juan, Instituto Nacional de Tecnología Agropecuaria (INTA), Calle 11 y Vidart, Pocito, San Juan J5427DEV, Argentina; roqueiro.gonzalo@inta.gob.ar
3 Facultad de Ingeniería (FI-UNSJ), Universidad Nacional de San Juan, Av. Lib. San Martín (Oeste) 1109, San Juan J5400ARY, Argentina
4 Institute of Environmental Assessment and Water Research (IDAEA)–CSIC, Jordi Girona 18-26, 08034 Barcelona, Spain; brian.young@idaea.csic.es
5 Instituto de Microbiología y Zoología Agrícola (IMYZA), Instituto Nacional de Tecnología Agropecuaria (INTA), Nicolás Repetto 2751, Hurlingham B1686HVU, Argentina
6 Instituto de Química San Luis (INQUISAL-CONICET), Chacabuco y Pedernera s/n, San Luis D5700BWS, Argentina; ppacheco@unsl.edu.ar
7 Departamento de Biodiversidad y Biología Experimental (DBBE), Facultad de Ciencias Exactas y Naturales-Universidad de Buenos Aires, Pabellón II, 4to Piso—Ciudad Universitaria, Ciudad Autónoma de Buenos Aires C1428BFA, Argentina; hernan@bg.fcen.uba.ar
8 Fundación Miguel Lillo, Instituto de Morfología Vegetal, Calle Miguel Lillo 251, San Miguel de Tucumán, Tucumán T4000JFF, Argentina; mimercado@lillo.org.ar
* Correspondence: heredia.belen@inta.gob.ar; Tel.: +54-(264)-492-1079 (ext. 1191)

Abstract

Growing concern over soil degradation and the demand for sustainable solutions have driven research into remediation technologies. This study aimed to evaluate the morphological, physiological, and phytochemical responses of *Larrea cuneifolia*, *Bulnesia retama*, *Plectrocarpa tetracantha*, and *Neltuma flexuosa* seedlings exposed to mining waste contaminated soil during early developmental stages. Plants were cultivated for 90 days in soils amended with increasing concentrations of mining waste. Higher waste proportions resulted in a dose-dependent increase in metal(loid)s concentrations and soil acidification. All species survived in soils containing up to 1572.6 mg kg^{-1} As, 25.6 mg kg^{-1} Cu, 33.0 mg kg^{-1} Cd, and 742.6 mg kg^{-1} Zn. Metal(loid)s accumulation occurred predominantly in roots, reaching 1895.1 mg kg^{-1} Zn in *P. tetracantha* and 2223.2 mg kg^{-1} As in *B. retama*. The presence of metal(loid)s in leaf and stem tissues was confirmed by SEM-EDX analysis. Elevated MDA levels, combined with low POX and APX activities, indicated a limited antioxidant response. Additionally, the abundance of yeast and bacterial colonies increased across all soil treatments associated with the studied native species. These results demonstrate remarkable tolerance of native species to multi-metal contamination and underscore their potential for cost-effective, nature-based strategies to restore mining-impacted soils in arid regions.

Keywords: metal; metalloid; oxidative stress; SEM-EDX; bioaccumulation; remediation; plants; chronic toxicity; microorganisms

Academic Editors: Meng Li and Sicheng Shao

Received: 23 December 2025
Revised: 5 February 2026
Accepted: 7 February 2026
Published: 1 March 2026

1. Introduction

Social concern over soil degradation and the demand for sustainable products and services have promoted the study and implementation of remediation technologies. In this context, metal(loid) contamination derived from anthropogenic activities has emerged as a major environmental problem, impacting ecosystem integrity and multiple life forms [1–3]. Mining represents one of the primary industrial activities responsible for generating large volumes of waste containing high concentrations of metal(loid)s [4]. Although certain metals (e.g., Cu, Zn, Cr, and Mn) play essential roles in physiological and biochemical processes of living organisms, concentrations exceeding optimal thresholds can induce toxic effects. In contrast, other elements such as Cd, As, and Pb can cause severe damage even at very low concentrations [5].

Numerous soil remediation strategies have been developed to address soil contamination, including incineration, soil washing, and vitrification, among others. However, physicochemical approaches involve higher costs, a greater environmental impact, limited efficiency at low contamination levels, and constraints when applied over large areas, frequently leading to the loss of soil productivity [6]. An alternative approach involves the use of plants (phytoremediation) and microorganisms (bioremediation), which enables soil recovery in a non-invasive and cost-effective manner while preserving the environmental viability of the remediated soil [7,8]. The effectiveness and type of phytoremediation strategy applied depend on plant species' responses to contaminants (e.g., phytostabilization, phytoextraction, and phytovolatilization), the bioavailability of toxic elements in the soil, and interaction with rhizosphere microorganisms. Plant growth rate, root system biomass production, ease of establishment, and tolerance to environmental stressors are key traits influencing the phytoremediation process [8]. Therefore, the successful implementation of in situ phytoremediation requires evaluating morphological, physiological, and biochemical plant responses during early developmental stages under different concentrations of metal(loid)s [9].

Processes occurring during the early stages of plant growth and species establishment are highly sensitive to the presence of contaminants. Metal(loid)s can induce phytotoxicity, leading to alterations in growth, vigor, development, productivity, and survival [10]. At the biochemical level, metal exposure promotes the excessive production of reactive oxygen species (ROS), causing damage to cell membranes and organelles, and potentially leading to cell death [11]. Despite these adverse effects, some plant species are able to survive and reproduce in environments with high metal(loid) concentrations. Such species have developed a series of tolerance mechanisms that mitigate the stress induced by various toxic elements. Plants also possess enzymatic antioxidant defenses (involving the increased activity of enzymes such as catalases, peroxidases, and superoxide dismutase), and non-enzymatic systems, characterized by the production of phenolic [12,13]. In addition, secondary metabolites and osmolytes, such as polysaccharides and polypeptides, contribute to the complexation of toxic elements, preventing damage by binding to the [14,15].

Understanding the mechanisms underlying metal(loid) tolerance and accumulation in different plant species with remediation potential is essential for the successful application of phytoremediation strategies [16]. Beyond the physiological and molecular mechanisms inherent to plants [17], the rhizosphere and its associated microorganisms play a crucial role in regulating metal tolerance and accumulation [18]. These microorganisms closely interact with plants, establishing associations that can significantly improve the phytoremediation process [19]. Consequently, the study of rhizosphere microbial communities provides an opportunity to understand plant responses to abiotic stress and offers the potential to enhance phytoremediation efficiency [19].

In the department of Caucete, San Juan province, Argentina, an abandoned gold mine has generated a contamination plume resulting from the accumulation of mining waste [20]. Heredia et al. [4] identified four native species in situ, *Neltuma flexuosa* (DC.) C.E. Hughes & G.P. Lewis (Fabaceae), *Larrea cuneifolia* Cav., *Plectrocarpa tetracantha* Gillies ex Hook. & Arn., and *Bulnesia retama* (Gillies ex Hook. & Arn.) Griseb. (Zygophyllaceae), all capable of bioaccumulating As, Cu, Cd, and Zn. These species, typical of arid environments, have developed morphological, biochemical and physiological strategies to cope with environmental stressors such as salinity and water deficit [21]. In the search for more suitable alternatives for the implementation of in situ phytoremediation strategies, this study aimed to (a) evaluate how *L. cuneifolia*, *B. retama*, *P. tetracantha*, and *N. flexuosa* respond to mining waste amended soils under chronic exposure, (b) determine the morphological, physiological, and biochemical responses of these four species to increasing metal(loid) concentrations and (c) evaluate the associated soil microbiological responses.

2. Materials and Methods

2.1. Seed and Soil Sampling

Soil and seed samples were collected in the locality of La Planta town, Caucete Department, San Juan Province, Argentina (Figure 1), at the site of a former gold processing plant. Gold extraction operations, involving rock processing and ore transport from nearby mining deposits, were active until 1960. After this date, activity ceased and no closure plans or mitigation measures were implemented, resulting in the formation of a contamination plume [4,20]. Within this area, Heredia et al. [4] identified and characterized two sites: Site 1 (S1), characterized by high concentrations of Cu, Cd, Zn, and As; and Site 2 (S2), which serves as a reference site, where metal(loid) concentrations comply with the regulatory thresholds established for residential and agricultural use (Federal Law 24.051).

For the chronic exposure bioassay, seeds of the four selected native bioaccumulator species [4] were collected from the study area—*Larrea cuneifolia* (a xerophytic shrub with perennial leaves and a woody stem, reaching up to 2 m in height; endemic to Argentina, distributed throughout the Monte Biogeographic Province, extending from northern Argentina to northern Patagonia, up to 3000 m a.s.l.), *Bulnesia retama* (a shrub reaching up to 3 m, characterized by branches and young stems covered by a waxy white layer; in Argentina, it is typical of the Monte Biogeographic Province, occurring between 500 and 2500 m a.s.l; it is also abundant in a restricted enclave in the semideserts of Ica, Ingenio, and Nazca in Peru), *Plectrocarpa tetracantha* (a shrub up to 2 m tall with propagative roots and perennial leaves; endemic to Argentina, inhabiting saline soils of the Monte Biogeographic Province, between 390 and 1200 m a.s.l.), and *Neltuma flexuosa* (a deciduous, thorny tree with deep root system, es up to 10 m tall; native to northern Chile and Argentina and characteristic of western arid zones and the Monte Biogeographic province).

Composite soil samples, each consisting of five subsamples, were collected from S1 and S2 at a depth of 0–20 cm. Prior to analysis and experimental setup, the soil samples were homogenized, air-dried at room temperature, and sieved through a 2 mm mesh.

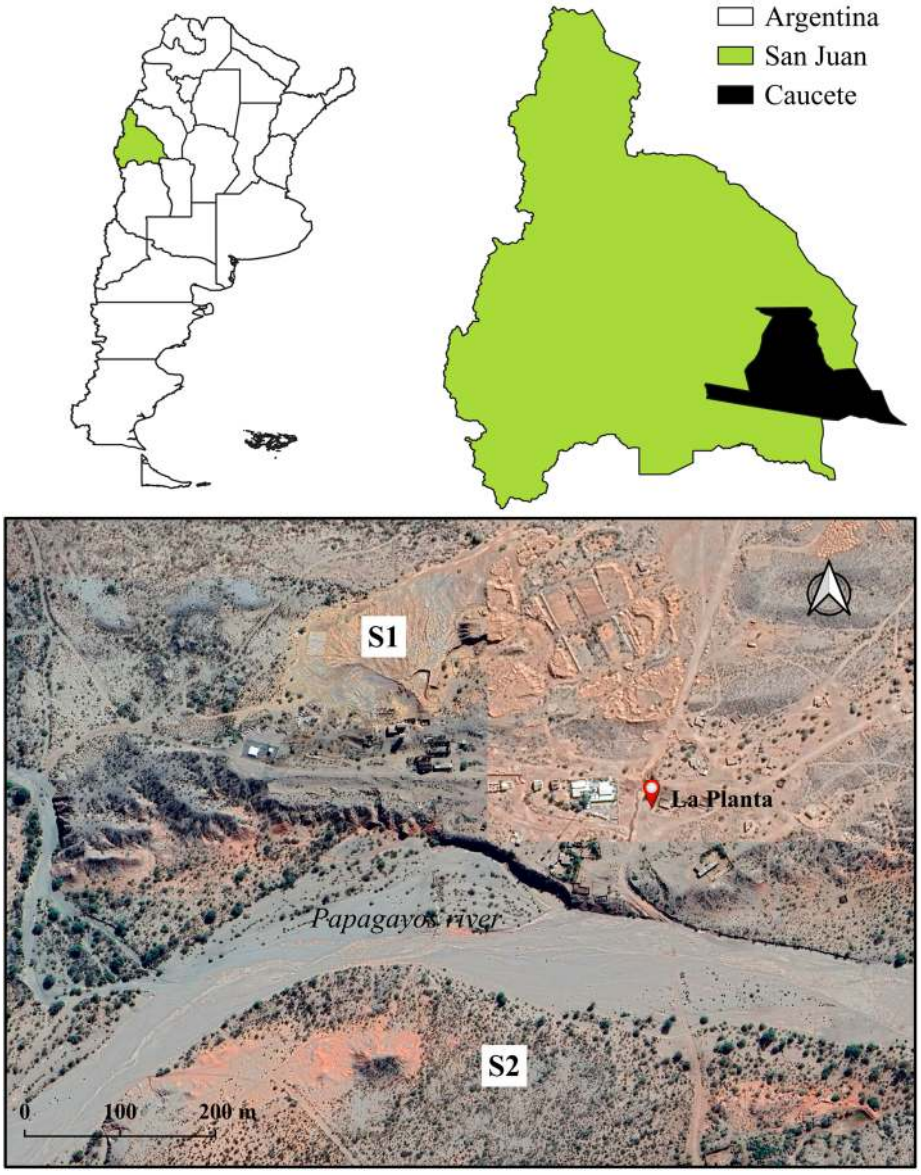

Figure 1. Study area in La Planta town, Caucete Department, San Juan Province, Argentina. Soil and seed sampling sites. S1: soil contaminated with mining waste and S2: reference soil.

2.2. Experimental Design and Growth Conditions

Seeds of the four species were germinated in a peat–perlite substrate and grown for 90 days under natural light and controlled temperature conditions in a greenhouse. After this period, the seedlings were transplanted into pots containing different proportions of mining waste. The pots were maintained in the greenhouse under natural light under ambient temperature conditions (Supplementary Materials, Figure S1), for an additional 90 days. Plants were irrigated regularly to maintain adequate soil moisture.

A completely randomized design was employed, comprising five soil treatments generated by the mechanical mixing of S1 and S2 soils at different proportions as follows: 0% S1 (T_0), 1% S1 (T_1), 10% S1 (T_{10}), 50% S1 (T_{50}), and 100% S1 (T_{100}). Ten replicates were established per treatment for each species, yielding a total of 50 experimental units per species. Each experimental unit consisted of one seedling was cultivated in 900 g of the corresponding soil mixture. An automated drip irrigation system with a flow rate of 4 L h^{-1} was installed. Fertilization was performed at 30-day intervals with 100 mL per plant of a YaraMila Hidrocomplex 12(N)-11(P)-18(K) solution (75 mg L^{-1}).

2.2.1. Soil Analysis and Contamination Indices

Soil physicochemical parameters, including pH (paste), electrical conductivity (saturated extract), and total and soluble concentrations of metal(loid)s, were determined for all treatments (T_0, T_1, T_{10}, T_{50}, and T_{100}) at the beginning and end of the assay. Total and soluble concentrations of metal(loid)s (Cu, Cd, Zn, and As) were measured according to Heredia et al. [4] using ICP-MS (detection limit 0.001 mg kg^{-1}).

Soil samples were digested using a Milestone Start-D microwave digester (Sorisole, Italy) to obtain the total metal(loid) fraction. A soil aliquot of 0.25 g was digested with 4 mL of 65% HNO_3, 1 mL of 30% H_2O_2, and 3 mL of 40% HF in a PTFE reactor. The digestion program consisted of a gradual temperature increase to 200 °C over 10 min, followed by a 20 min hold. Microwave power reached 1000 W. The resulting extracts were used for metal(loid) determination.

To obtain the soluble fraction, soil samples were mixed with deionized water in a 1:4 (w/v) ratio for 30 min, and the supernatant was filtered after an additional 60 min. The resulting supernatant was used for the determination of soluble metal(loid)s [22].

Soil contamination levels were evaluated by calculating the Contamination Factor (CF; Equation (1)) for each metal(loid) and the overall Contamination Degree (Cdeg; Equation (2)) [23].

$$CF = \frac{MC}{RC} \quad (1)$$

where MC is the concentration of a particular metal(loid) in T_1, T_{10}, T_{50}, and T_{100}, and RC is the concentration of the same metal(loid) in soil from the reference site (T_0).

$$C_{deg} = \sum CF \quad (2)$$

where C_{deg} is the sum of the calculated CF values.

2.2.2. Determination of Metal(loid) Concentrations in Plant Tissues and Bioaccumulation Indices

After 90 days of exposure, three individuals per treatment for each species were harvested and separated into aerial parts and roots. The samples were washed with tap water to remove soil particles and subsequently rinsed with deionized water [24]. Plant material was then dried at 70 °C for 48 h and ground using a high-speed universal disintegrator (Model FW100). The ground material was macerated and digested with an acid mixture, following the methodology described by Heredia et al. [4]. Briefly, a 0.05 g subsample was digested with 1 mL of HNO_3 and 0.5 mL of H_2O_2, in a thermal bath at 60 °C for 90 min, after which 100 µL of HF was added. Finally, digested samples were diluted to a final volume of 6 mL with Milli Q water and centrifuged at 1250 rpm for 5 min. Metal(loid) concentrations were determined by ICP-MS (detection limit 0.001 mg kg^{-1}).

The bioaccumulation factor (BAF) and translocation factor (TF) for Cu, Cd, Zn, and As were calculated [25]. BAF was defined as the ratio between the concentration of each metal(loid) in plant organs (leaves, stems, and roots) and its total concentration in the soil. TF was calculated as the ratio between the concentration of a specific metal(loid) in aerial organs (leaves and stems) and its concentration in the roots.

2.2.3. Plant Morpho-Physiological Parameters

Morphological parameters were evaluated at 15, 45, and 75 days of exposure, including: stem height, stem basal diameter (BD), number of damaged leaves (defined as those exhibiting chlorosis or necrosis in more than 50% of the total leaf area), and the number of green leaves. At the end of the exposure period, stem and root dry weights were

determined. In addition, the no observed effect concentration (NOEC), lowest observed effect concentration (LOEC), and the 50% inhibitory concentration (IC50) were estimated.

2.3. Oxidative Stress Biomarkers

2.3.1. Ascorbate Peroxidase (APX) and Guaiacol Peroxidase (POX) Activity

APX and POX activities were determined according to Roqueiro et al. [12]. Enzyme extraction was performed by grinding 100 mg of aerial plant tissue in liquid nitrogen with 0.05 M potassium phosphate buffer (pH 7). The homogenate was centrifuged at 12,000 *g* at 4 °C for 30 min, and the supernatant was collected for analysis.

For APX activity, the reaction mixture consisted of 390 µL of 50 mM phosphate buffer (pH 7), 40 µL of plant extract, 60 µL of ascorbic acid, and 10 µL of H_2O_2. Absorbance was recorded at 290 nm.

For POX activity, the reaction mixture contained 30 µL of plant extract, 410 µL of 150 mM potassium phosphate buffer (pH 6.1), 50 µL of guaiacol, and 10 µL of H_2O_2. Absorbance was measured at 470 nm.

Enzymatic activities were determined using a Thermo Scientific NanoDrop spectrophotometer and expressed relative to protein content determined by the Bradford [26].

2.3.2. Lipid Peroxidation

Malondialdehyde (MDA) content was determined, following the Heath and Packer [27] protocol. Briefly, 50 mg of each sample was homogenized in 80% ethanol and centrifuged at 12,000 *g*. An aliquot of 200 µL of the supernatant was mixed with 200 µL of thiobartbituric acid (TBA) reagent TBA (0.5% TBA in 20% trichloroacetic acid, TCA). The mixture was then centrifuged at 10,000 *g* and incubated in a water bath at 80 °C. After cooling at room temperature, absorbance was measured at 490 and 630 nm using a microplate spectrophotometer (BioTek). MDA concentration was estimated using Equation (3).

$$\mathrm{MDA} = \mathrm{Abs}_{490} - \mathrm{Abs}_{630}/(\varepsilon \cdot l) \quad (3)$$

where Abs is the absorbance recorded at the wavelength indicated in the subscript, ε is the molar extinction coefficient of MDA (155,000 mM^{-1} mL^{-1}), and l is the optical well pitch of the microplate (0.82 cm for a 300 µL volume).

2.4. Colony-Forming Unit (CFU) Count

Soil samples were collected at the beginning and the end of the chronic exposure period and stored at 4 °C for the determination of colony-forming units (CFUs). Microorganism abundance was quantified following standard serial dilution and plate counting techniques [28]. Three serial dilutions were prepared in triplicate, and 100 µL aliquots were spread plated onto 9 mm Ø Petri dishes containing enriched culture media for bacterial and yeast growth. The plates were incubated at 30 °C for 24 h and 48 h for bacteria and yeast counts, respectively.

2.5. Scanning Electron Microscopy and Energy Dispersive X-Ray Spectroscopy (SEM-EDX)

At the end of the exposure period, fresh leaves, stems, and roots were sampled from three individuals per treatment and for each species. Transverse sections of each organ, approximately 3 mm thick, were obtained by free-hand sectioning using a stainless-steel razor blade. The sections were mounted on aluminum stubs using double-sided carbon tape and subsequently analyzed without coating by scanning electron microscopy (SEM) coupled with energy dispersive X-ray detector (EDX) using a Zeiss Supra55VP microscope. The equipment was operated under variable pressure (VP, 20–40 Pa) at the Centro Integral de Microscopía Electrónica (CIME, CONICET-UNT), Tucumán, Argentina.

2.6. Data Analysis

One-way analysis of variance (ANOVA) was used to evaluate differences among treatments for the physiological, morphological, and biochemical variables. Tukey's test was applied for post hoc comparisons. When data did not meet the assumptions of normality or homoscedasticity, nonparametric Kruskal–Wallis tests were employed, and, where necessary, data were transformed using arcsine square root or logarithmic transformations. Spearman correlation analyses were performed to examine the relationships among physiological variables, BAF, and the percentage decrease in metal(loid)s in the soil. Statistical analyses were performed using R software (version 4.3.0), and graphs were generated using GraphPad Prism 5 software.

3. Results

3.1. Soil Parameters

3.1.1. Soil Physicochemical Variables and Contamination Indexes

Increasing the proportion of mining waste across treatments resulted in increased metal(loid) content and progressive soil acidification. In the more concentrated treatments (T_{50} and $T1_{00}$), soil pH values ranged from 4.2 to 4.3 (Table 1). Bacterial and yeast CFUs decreased by 90 to 100% in treatments T_{50} and T_{100}. Regarding soil contamination indices, the CF from T_{10} onwards was classified into the highest contamination category, "high to very high contamination factor", for all four studied metal(loid)s. Similarly, the C_{deg} from T_1 to T_{100} fell within the two highest categories, "high and very high degree of contamination" (Table S1).

Table 1. Initial physicochemical and microbiological characterization of each treatment.

Concentration of Metal(loid)s in Total and Soluble Fractions (mg kg^{-1})									pH	EC (mS cm^{-1})	CFU (g^{-1} mL^{-1})	
Treatment	**As**		**Cu**		**Cd**		**Zn**					
	Total	**Soluble**	**Total**	**Soluble**	**Total**	**Soluble**	**Total**	**Soluble**			**Bacteria**	**Yeasts**
T_0	14.3	0.1	7.9	0.03	0.9	0.0	63.3	0.1	7.5	0.1	$1.37 \times 10^{+6}$	$5.5 \times 10^{+4}$
T_1	84.1	0.2	22.3	0.03	2.7	0.0	245.1	0.3	7.7	0.5	$5.7 \times 10^{+5}$	$6.0 \times 10^{+4}$
T_{10}	1572.6	0.1	27.9	0.03	33.0	0.2	1032.3	0.2	7.8	1.7	$9.45 \times 10^{+5}$	$7.0 \times 10^{+4}$
T_{50}	5178.8	0.2	114.0	nd	231.3	4.5	4083.3	0.2	4.3	5.0	nd	$1.0 \times 10^{+4}$
T_{100}	7322.1	0.2	226.2	nd	328.9	3.0	5677.6	0.2	4.2	4.4	$1.5 \times 10^{+4}$	$5.0 \times 10^{+3}$

EC: electrical conductivity; CFUs: colony-forming units; nd: not detected.

At the end of the seedling exposure period, total and soluble metal(loid) concentrations were determined for each treatment. Copper concentration in the rhizosphere soil of *L. cuneifolia* and *N. flexuosa* did not differ between T_0 and T_1. Similarly, Cd concentration in the rhizosphere soil of *B. retama* and *N. flexuosa* also showed no statistically significant differences between T_0 and T_1. Finally, Zn concentrations in the rhizosphere soil of *P. tetracantha* and *N. flexuosa* did not differ between T_0 and T_1 ($p > 0.05$) (Table S2).

Comparisons between initial and final soil metal(loid) concentrations revealed significant decreases, indicating removal or immobilization during plant growth (Figure 2). The presence of native species resulted in reductions ranging from 5% to 70% in T_1, with Cu and Zn showing the greatest decreases and As exhibiting the lowest reduction percentage. In T_{10}, the reduction percentages ranged between 10% and 60%, with As showing the highest percentage of decrease relative to its initial concentration.

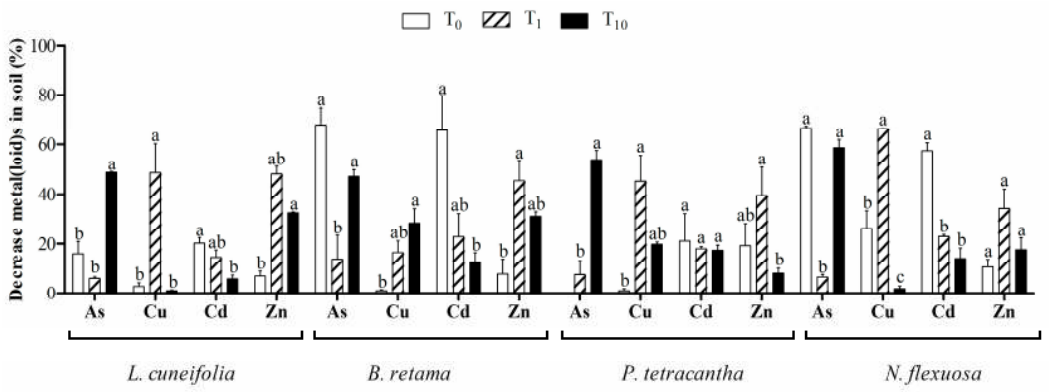

Figure 2. Mean percentage of total metal(loid) decrease (±SE) relative to the initial soil concentration, for each treatment. Different letters indicate significant differences between treatments for each species ($p < 0.05$).

3.1.2. Colony-Forming Units (CFUs)

Due to the total mortality of seedlings in treatments T_{50} and T_{100}, microbial abundance was exclusively analyzed in the rhizosphere soil of treatments T_0, T_1, and T_{10}. Figure 3 shows the percentage of variation in microbial abundance at the end of the exposure period compared to the initial counts at the beginning of the experiment. An increase of over 20% was recorded for both bacteria and yeasts throughout the experiment across all treatments and plant species evaluated. For most species, the percentages of increase did not differ significantly among treatments ($p > 0.05$), except for *N. flexuosa*, which showed a significantly lower increase in yeast CFUs in T_{10} ($p < 0.02$) compared to T_0 and T_1. The maximum increased bacterial CFU (251%) was obtained for *L. cuneifolia* in T_1 compared to T_0, while yeast CFUs showed the highest increase (225%) in the rhizosphere soil of *N. flexuosa* in T_{10}.

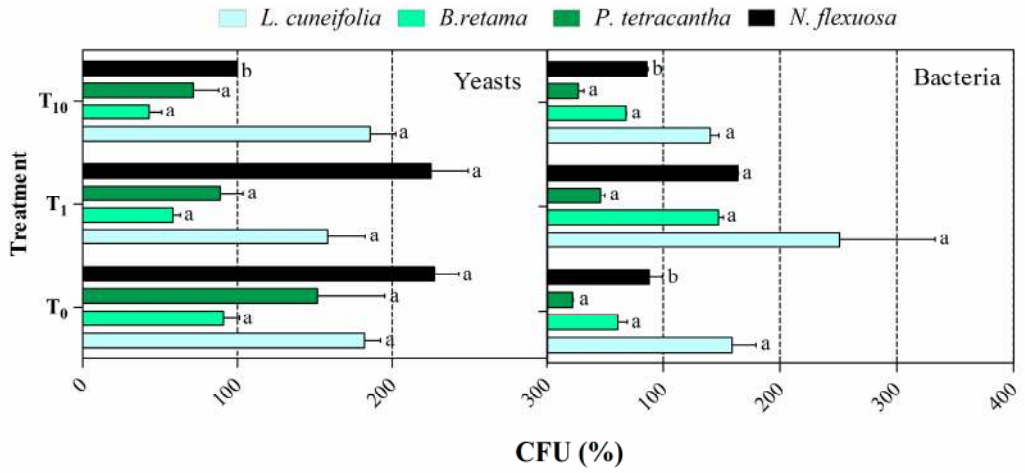

Figure 3. Percentage change (± SE) in colony-forming units (CFUs) from initial to final soil conditions for each treatment and species. Different letters indicate significant differences between treatments for each species ($p < 0.05$). Reference: initial values, bacteria: T_0 (0% mining waste): 1.37×10^6 g^{-1} mL^{-1}; T_1 (1% mining waste): 5.7×10^5 g^{-1} mL^{-1}; and T_{10} (10% mining waste): 9.5×10^5 g^{-1} mL^{-1}. Yeasts: T_0: 5.5×10^4 g^{-1} mL^{-1}; T_1: 6.0×10^4 g^{-1} mL^{-1}; and T_{10}: 7.0×10^4 g^{-1} mL^{-1}.

3.2. Mopho-Physiological Parameters

Under treatments T_{50} and T_{100}, all four plant species evaluated exhibited 100% mortality within the first 15 days of exposure, indicating acute toxicity. Therefore, morpho-physiological variables were assessed only in treatments T_0, T_1, and T_{10}.

The stem BD and height were not significantly affected by the increasing proportions of contaminated soil during the first 45 days of exposure ($p > 0.05$). However, after 90 days, T_{10} exerted a significant impact on all mopho-physiological variables evaluated ($p < 0.01$) (Table 2).

All species showed a time-dependent response in the number of green and symptomatic damaged leaves after 45 days of exposure ($p < 0.001$). A marked increase in chlorotic and necrotic leaves was observed in $T_{10,}$ with a corresponding decrease in the number of green leaves. Aerial dry biomass was highest in T_1, reaching a maximum of 2.0 g in *N. flexuosa*, while in T_{10}, aerial dry biomass production for all species was below 1.0 g (Table 2). The root dry biomasses of *B. retama* did not differ among treatments ($p > 0.05$). Conversely, in other species, the highest dry root dry biomass production was recorded in T_0 and T_1, with a significant decrease in T_{10} ($p < 0.05$). After 90 days of exposure, the LOEC and NOEC values were 10% and 1%, respectively, for all assessed variables across the four species (Table S3).

3.3. Concentration of Metal(loid)s in Vegetative Organs

After 90 days of exposure, the metal(loid) concentrations were determined in roots and aerial organs (leaves and stems) (Table 3). In *L. cuneifolia*, higher concentrations of As, Cu, and Cd were detected in the roots of individuals exposed to T_{10} ($p < 0.05$). In contrast, Zn was predominantly accumulated in the aerial organs of individuals exposed to T_1 and T_{10} ($p < 0.05$), reaching an average concentration of 1496.0 mg kg^{-1} in plants exposed to T_1.

In *B. retama*, Cd was detected exclusively in the roots. This species exhibited higher concentrations of As, Cu, and Cd in roots under T_{10} ($p < 0.01$), with As reaching 2223.2 mg kg^{-1}. In aerial organs, metal(loid) concentrations followed a similar pattern to that recorded in roots, with higher concentrations of As, Cu, and Cd in T_{10} ($p < 0.05$), while Zn was more concentrated in T_1 ($p < 0.001$) for *B. retama* and *P. tetracantha*. In *P. tetracantha*, Zn reached values of 1895.1 mg kg^{-1} in the roots of individuals exposed to T_1. Similarly, the highest metal(loid) concentrations in *N. flexuosa* were recorded in the roots of plants exposed to T_1, with Zn reaching 1619.8 mg kg^{-1}. Regarding the aerial organs, individuals exposed to T_{10} exhibited higher concentrations of As and Cd, while Zn accumulation reached its maximum in T_1 plants ($p < 0.05$).

Bioaccumulation (BAF) and Translocation (TF) Factors

The highest BAF values were recorded in the roots of all four studied species (Figure 4). Notably, BAF values of 50 and 48 were observed for Cu in the roots of *L. cuneifolia* and *B. retama* exposed to T_1 and T_{10}, respectively. A BAF value of 20 for Cd was recorded in the roots of *P. tetracantha* exposed to $T_{1,}$ while values of 10 and 9 were obtained for Zn and As, respectively, in the roots of *N. flexuosa* under T_1 ($p < 0.05$). In aerial organs, the highest BAF values were also recorded in plants exposed to T_1; however, the BAF did not exceed 12 for any of the metal(loid)s.

Table 2. Mean (±SE) of morpho-physiological parameters measured during the 90 days of exposure for each species. Different letters indicate significant differences between treatments for each species ($p < 0.05$).

Parameter	Plant Species											
	Larrea cuneifolia			*Bulnesia retama*			*Plectrocarpa tetracantha*			*Neltuma flexuosa*		
	T_0	T_1	T_{10}	T_0	T_1	T_{10}	T_0	T_1	T_{10}	T_0	T_1	T_{10}
Stem height (mm)												
15 days	32.1 ± 5.7 ^{a}	48.2 ± 4.6 ^{a}	38.7 ± 3.2 ^{a}	81.4 ± 9.4 ^{a}	83.6 ± 6.3 ^{a}	80.9 ± 9.4 ^{a}	66.7 ± 12.8 ^{a}	61.6 ± 3.1 ^{a}	51.0 ± 4.3 ^{a}	68 ± 5.6 ^{ab}	75.9 ± 4.2 ^{a}	57.0 ± 3.0 ^{b}
45 days	50.9 ± 8.3 ^{a}	73.8 ± 5.8 ^{a}	46.8 ± 9.0 ^{a}	126.4 ± 11.2 ^{a}	133.8 ± 10.3 ^{a}	111.0 ± 13.9 ^{a}	112.5 ± 16.2 ^{a}	116.9 ± 5.8 ^{a}	71.3 ± 5.0 ^{b}	110.3 ± 10.8 ^{a}	127.1 ± 7.3 ^{a}	72.5 ± 6.2 ^{b}
75 days	78.6 ± 2.2 ^{a}	104.4 ± 8.3 ^{a}	71.4 ± 13.7 ^{a}	213.0 ± 9.9 ^{ab}	266.6 ± 32.2 ^{a}	174.2 ± 18.2 ^{b}	234.8 ± 28.5 ^{a}	241.7 ± 27.2 ^{a}	92.3 ± 16.6 ^{b}	241.0 ± 36.6 ^{b}	361.2 ± 18.1 ^{a}	84.9 ± 8.3 ^{c}
BD (mm)												
15 days	1.1 ± 0.2 ^{a}	1.2 ± 0.1 ^{a}	1.2 ± 0.1 ^{a}	2.0 ± 0.2 ^{a}	2.0 ± 0.1 ^{a}	2.0 ± 0.1 ^{a}	1.6 ± 0.1 ^{a}	1.6 ± 0.2 ^{a}	1.4 ± 0.1 ^{a}	1.5 ± 0.1 ^{a}	1.6 ± 0.2 ^{a}	1.5 ± 0.1 ^{a}
45 days	1.0 ± 0.1 ^{b}	1.4 ± 0.1 ^{a}	1.0 ± 0.1 ^{b}	2.0 ± 0.1 ^{a}	2.1 ± 0.1 ^{a}	2.1 ± 0.1 ^{a}	1.4 ± 0.1 ^{a}	1.4 ± 0.1 ^{a}	1.5 ± 0.1 ^{a}	1.5 ± 0.1 ^{a}	1.5 ± 0.1 ^{a}	1.4 ± 0.1 ^{a}
75 days	1.7 ± 0.1 ^{b}	2.1 ± 0.0 ^{a}	1.3 ± 0.2 ^{b}	2.2 ± 0.1 ^{a}	2.4 ± 0.1 ^{a}	2.1 ± 0.1 ^{a}	2.1 ± 0.1 ^{a}	2.2 ± 0.1 ^{a}	1.5 ± 0.1 ^{b}	1.9 ± 0.1 ^{ab}	2.3 ± 0.2 ^{a}	1.5 ± 0.1 ^{b}
Green leaves (n°)												
15 days	9.1 ± 2.4 ^{a}	14.9 ± 2.4 ^{a}	10.3 ± 1.6 ^{a}	9.9 ± 2.0 ^{a}	8.4 ± 1.0 ^{a}	11.1 ± 1.1 ^{a}	11.2 ± 1.1 ^{a}	10.8 ± 1.0 ^{a}	9.5 ± 1.0 ^{a}	4.8 ± 1.0 ^{a}	6.4 ± 1.0 ^{a}	5.0 ± 1.0 ^{a}
45 days	15.6 ± 3.3 ^{a}	25.3 ± 3.1 ^{a}	5.4 ± 1.4 ^{b}	18.9 ± 2.2 ^{a}	20.0 ± 1.1 ^{a}	7.3 ± 1.6 ^{b}	16.5 ± 2.0 ^{a}	17.5 ± 1.0 ^{a}	9.0 ± 1.5 ^{b}	9.3 ± 1.8 ^{a}	10.0 ± 1.3 ^{a}	1.8 ± 1.0 ^{b}
75 days	48.3 ± 7.5 ^{a}	76.0 ± 5.8 ^{a}	12.3 ± 6.4 ^{b}	45.3 ± 4.1 ^{a}	47.8 ± 3.8 ^{a}	5.7 ± 1.0 ^{b}	31.3 ± 2.5 ^{b}	49.0 ± 5.7 ^{a}	8.5 ± 3.6 ^{c}	13.6 ± 1.4 ^{b}	23.0 ± 1.3 ^{a}	1.0 ± 0.4 ^{c}
Damaged leaves (n°)												
15 days	1.0 ± 0.5 ^{a}	1.0 ± 0.5 ^{a}	1.1 ± 0.5 ^{a}	0.4 ± 0.3 ^{a}	0.1 ± 0.0 ^{a}	0.4 ± 0.2 ^{a}	nd	0.3 ± 0.2 ^{a}	0.3 ± 0.2 ^{a}	1.0 ± 0.4 ^{a}	1.0 ± 0.4 ^{a}	1.4 ± 0.4 ^{a}
45 days	1.0 ± 0.5 ^{b}	0.4 ± 0.3 ^{b}	1.1 ± 0.5 ^{a}	1.0 ± 0.5 ^{b}	1 ± 0.3 ^{b}	7.6 ± 1.3 ^{a}	0.3 ± 0.2 ^{b}	1.2 ± 1.0 ^{ab}	3.3 ± 1.1 ^{a}	0.3 ± 0.2 ^{b}	0.3 ± 0.2 ^{b}	3.8 ± 0.4 ^{a}
75 days	1.0 ± 0.5 ^{b}	0.3 ± 0.1 ^{b}	15.3 ± 2.3 ^{a}	0.2 ± 0.1 ^{b}	1.0 ± 0.5 ^{b}	22.7 ± 2.3 ^{a}	nd	nd	6.0 ± 2.0	1.0 ± 0.4 ^{b}	0.2 ± 0.1 ^{b}	3.0 ± 1.0 ^{a}
Dry biomass (g)												
Aerial organs	0.7 ± 0.1 ^{b}	1.3 ± 0.1 ^{a}	0.2 ± 0.0 ^{c}	1.1 ± 0.1 ^{ab}	1.4 ± 0.1 ^{a}	1.0 ± 0.1 ^{b}	1.4 ± 0.2 ^{a}	1.4 ± 0.1 ^{a}	0.1 ± 0.0 ^{b}	1.2 ± 0.1 ^{a}	2.0 ± 0.3 ^{a}	0.1 ± 0.0 ^{b}
Root	0.3 ± 0.1 ^{ab}	0.4 ± 0.0 ^{a}	0.1 ± 0.0 ^{b}	0.3 ± 0.0 ^{a}	0.2 ± 0.0 ^{a}	0.3 ± 0.0 ^{a}	0.5 ± 0.1 ^{a}	0.5 ± 0.0 ^{a}	0.1 ± 0.0 ^{b}	1.0 ± 0.0 ^{a}	1.0 ± 0.1 ^{a}	0.1 ± 0.0 ^{b}

BD: diameter base steam; nd: not detected; T0: 0% mining waste; T1: 1% mining waste; T10: 10% mining waste; aerial organs: stems and leaves.

Table 3. Mean (±SE) concentration of metal(loid)s (mg kg^{-1}) for each species in vegetative organs (shoots and roots). Different letters indicate statistical differences between treatments for each species ($p < 0.05$).

Specie	As			Cu			Cd			Zn		
	T_0	T_1	T_{10}	T_0	T_1	T_{10}	T_0	T_1	T_{10}	T_0	T_1	T_{10}
L. cuneifolia												
Aerial organs	208.8 ± 46.3 ^{a}	275.1 ± 30.4 ^{a}	288.8 ± 0.9 ^{a}	45.6 ± 9.6 ^{a}	35.9 ± 0.9 ^{a}	37.5 ± 0.01 ^{a}	nd	nd	nd	629.0 ± 54.1 ^{b}	1496.0 ± 166.4 ^{a}	1212.4 ± 4.9 ^{ab}
Root	334.7 ± 33.3 ^{b}	511.6 ± 65.4 ^{b}	772.0 ± 2.1 ^{a}	273.7 ± 36.0 ^{b}	492.7 ± 111.0 ^{ab}	640.7 ± 2.9 ^{a}	23.4 ± 8.2 ^{c}	77.7 ± 5.9 ^{b}	236.6 ± 05 ^{a}	663.4 ± 85.0 ^{a}	8.9 ± 1.0 ^{c}	24.2 ± 0.0 ^{b}
B. retama												
Aerial organs	134.7 ± 27.8 ^{b}	211.3 ± 13.1 ^{ab}	219.9 ± 20.8 ^{a}	38.2 ± 4.6 ^{b}	68.4 ± 10.8 ^{ab}	109.0 ± 15.9 ^{a}	nd	11.1 ± 1.5 ^{b}	134.3 ± 7.2 ^{a}	413.1 ± 18.3 ^{a}	827.1 ± 37.4 ^{a}	13.3 ± 2.3 ^{b}
Root	162.1 ± 20.5 ^{b}	232.9 ± 4.1 ^{b}	2223.2 ± 2.1 ^{a}	167.4 ± 33.9 ^{b}	169.9 ± 27.8 ^{b}	946.9 ± 20.2 ^{a}	12.6 ± 2.2 ^{b}	25.6 ± 0.9 ^{b}	327.2 ± 10.0 ^{a}	958.6 ± 31.0 ^{a}	1018.1 ± 50.0 ^{a}	28.1 ± 6.3 ^{b}
P. tetracantha												
Aerial organs	109.0 ± 3.5 ^{c}	163.6 ± 8.3 ^{b}	280.4 ± 14.4 ^{a}	42.3 ± 2.6 ^{b}	79.9 ± 6.2 ^{b}	166.5 ± 14.6 ^{a}	nd	6.8 ± 1.3 ^{b}	274.1 ± 27.5 ^{a}	441.4 ± 78.8 ^{b}	1400.3 ± 190.6 ^{a}	29.3 ± 0.6 ^{c}
Root	187.7 ± 47.7 ^{b}	357.0 ± 71.7 ^{b}	712.5 ± 79.6 ^{a}	143.0 ± 18.1 ^{b}	209.6 ± 9.4 ^{ab}	296.2 ± 44.5 ^{a}	12.9 ± 0.6 ^{c}	45.9 ± 9.2 ^{b}	176.6 ± 31.0 ^{a}	368.4 ± 0.5 ^{b}	1895.1 ± 128.5 ^{a}	20.1 ± 2.2 ^{c}
N. flexuosa												
Aerial organs	198.0 ± 3.8 ^{b}	341.0 ± 32.2 ^{b}	676.0 ± 50.8 ^{a}	70.5 ± 9.3 ^{a}	79.1 ± 18.5 ^{a}	69.4 ± 10.4 ^{a}	6.7 ± 0.4 ^{b}	6.8 ± 0.5 ^{b}	277.5 ± 31.7 ^{a}	310.1 ± 1.2 ^{b}	564.3 ± 33.2 ^{a}	35.0 ± 3.5 ^{c}
Root	71.8 ± 9.9 ^{c}	711.5 ± 23.5 ^{a}	333.3 ± 43.1 ^{b}	177.1 ± 14.7 ^{a}	211.9 ± 6.2 ^{a}	81.6 ± 18.3 ^{b}	14.1 ± 0.1 ^{b}	11.4 ± 2.0 ^{b}	123.6 ± 16.7 ^{a}	581.1 ± 16.6 ^{b}	1619.8 ± 101.0 ^{a}	12.8 ± 1.3 ^{c}

nd: not detected; T_0: 0% mining waste; T_1: 1% mining waste; T_{10}: 10% mining waste; aerial organs: stems and leaves.

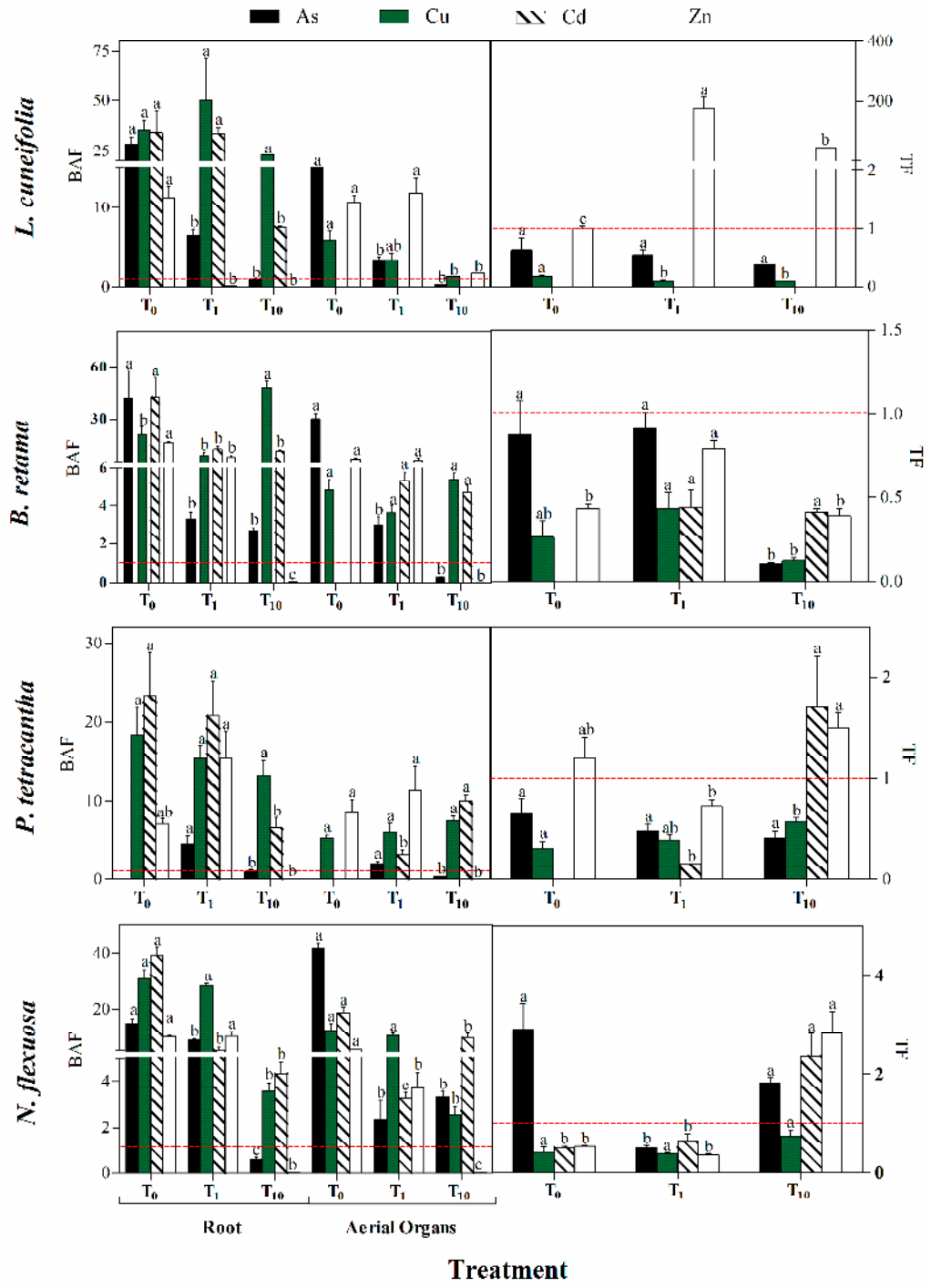

Figure 4. Mean (± SE) of the bioaccumulation factor (BAF) and translocation factor (TF) as a function of the total concentration of As, Cu, Cd, and Zn. Red line represents BAF values equal to 1. Different letters indicate statistical differences between treatments for specie ($p < 0.05$). Aerial organs: stems and leaves.

The TF across the four species ranged from 0.2 to 3 in T_1 and T_{10}, reaching values of 100 in T_1 for *L. cuneifolia*. Zn was the element with the highest translocation values in *B. retama*, *N. flexuosa*, and *L. cuneifolia*, while Cd showed the highest TF in *P. tetracantha*.

Correlation analyses between morpho-physiological variables measured at the end of the exposure period, bioaccumulation indices, and the decrease in soil metal(loid) concentrations revealed species-specific patterns (Figure 5). In *L. cuneifolia* stem, height ($R > -0.7$; $p < 0.05$) and number of green leaves ($R > -0.9$; $p < 0.001$) were strongly and negatively correlated with the reduction in As in the soil, whereas these same variables

were positively correlated with Cu reduction (stem height R > 0.7; $p < 0.05$ and green leaves R > 0.9; $p < 0.001$).

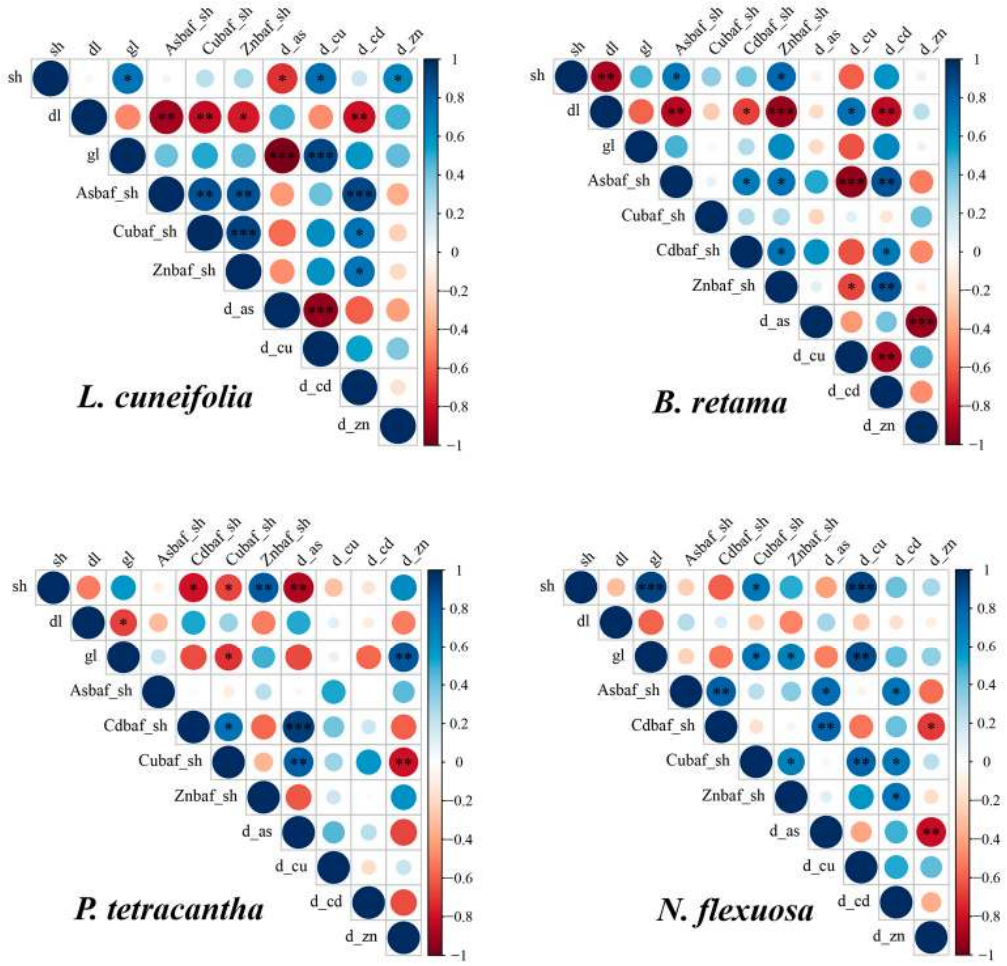

Figure 5. Spearman correlation matrix between the variables analyzed. The circles represent the strength and sign of the correlation: blue circles indicate positive correlations, and red circles indicate negative correlations, while the size of the circle is proportional to the absolute value of the correlation coefficient (r). Only statistically significant correlations ($p < 0.05$) are shown; non-significant correlations were omitted. The asterisks in the circles indicate the significance of the correlation (* $p < 0.05$; ** $p < 0.01$; *** $p < 0.001$). References: sh: shoot height; dl: damaged leaves; gl: green leaves; Metal(loid)baf_sh: bioaccumulation factor in shoots; d_metal(loid): percentage decrease in metal(loid) in soil.

In *B. retama*, BAF for As, Zn, and Cd in aerial organs correlated negatively with the number of damaged leaves (R > −0.7; $p < 0.001$). Percentages of decrease Cd/Cu and As/Zn in soil also showed a strong negative correlation (R > −0.8; $p < 0.001$). Similar patterns were observed in *N. flexuosa* and *P. tetracantha*. In *P. tetracantha*, Cu accumulation in aerial organs was negatively correlated with stem height and number of green leaves ($p < 0.05$). Moreover, *P. tetracantha* was the only species in which BAF and soil Cu reduction were negatively correlated with the measured morphological variables (Figure 5).

3.4. Oxidative Stress Biomarkers

Antioxidant Activity and Lipid Peroxidation

Figure 6 shows the results of the oxidative stress biomarkers. Although APX and POX activities increased by over 2% in T_1 compared to T_0, this increase was statistically

significant only for *N. flexuosa* ($p < 0.05$). In contrast, no significant differences were observed in *L. cuneifolia*, *P. tetracantha*, or *B. retama* ($p > 0.05$).

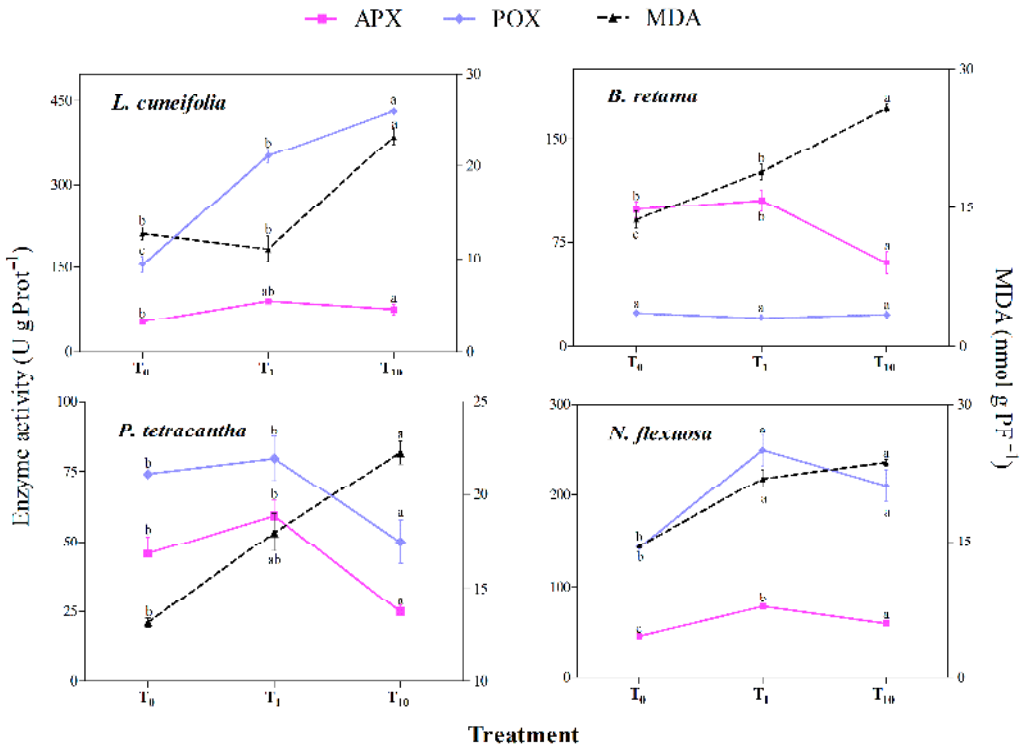

Figure 6. Mean (±SE) of oxidative stress biomarkers for the four species after 15 days of exposure to mining waste, APX: ascorbate peroxidase, POX: guaiacol peroxidase, MDA: malondialdehyde. Different letters indicate significant differences between treatments for species ($p < 0.05$).

A reduction in enzyme activity was observed in T_{10} ($p < 0.05$), except in *P. tetracantha*, where POX activity did not differ among treatments ($p > 0.05$). MDA levels increased in a dose-dependent manner with higher proportions of contaminated soil, reaching maximum levels in T_{10}, where antioxidant activity was reduced. Overall, treatments that showed enhanced antioxidant activity did not exhibit significant differences in MDA production compared to T_0 ($p > 0.05$).

3.5. Metal(loid) Histolocation

Leaf, stem, and root sections from individuals exposed to T_0 and T_{10} were analyzed by SEM-EDX (Figure 6 and Table S4). Under T_{10} conditions, Cu was detected in the xylem and phloem tissues of the stems, as well as in the mesophyll of *N. flexuosa* (Figure 7d,f). Similarly, Zn, As, and Pb were identified in the mesophyll of *L. cuneifolia* at T_{10}, while Pb was detected in the mesophyll of *B. retama* (Figure 7b,h). SEM-EDX data for *P. tetracantha* are not presented due to insufficient material available for the analysis.

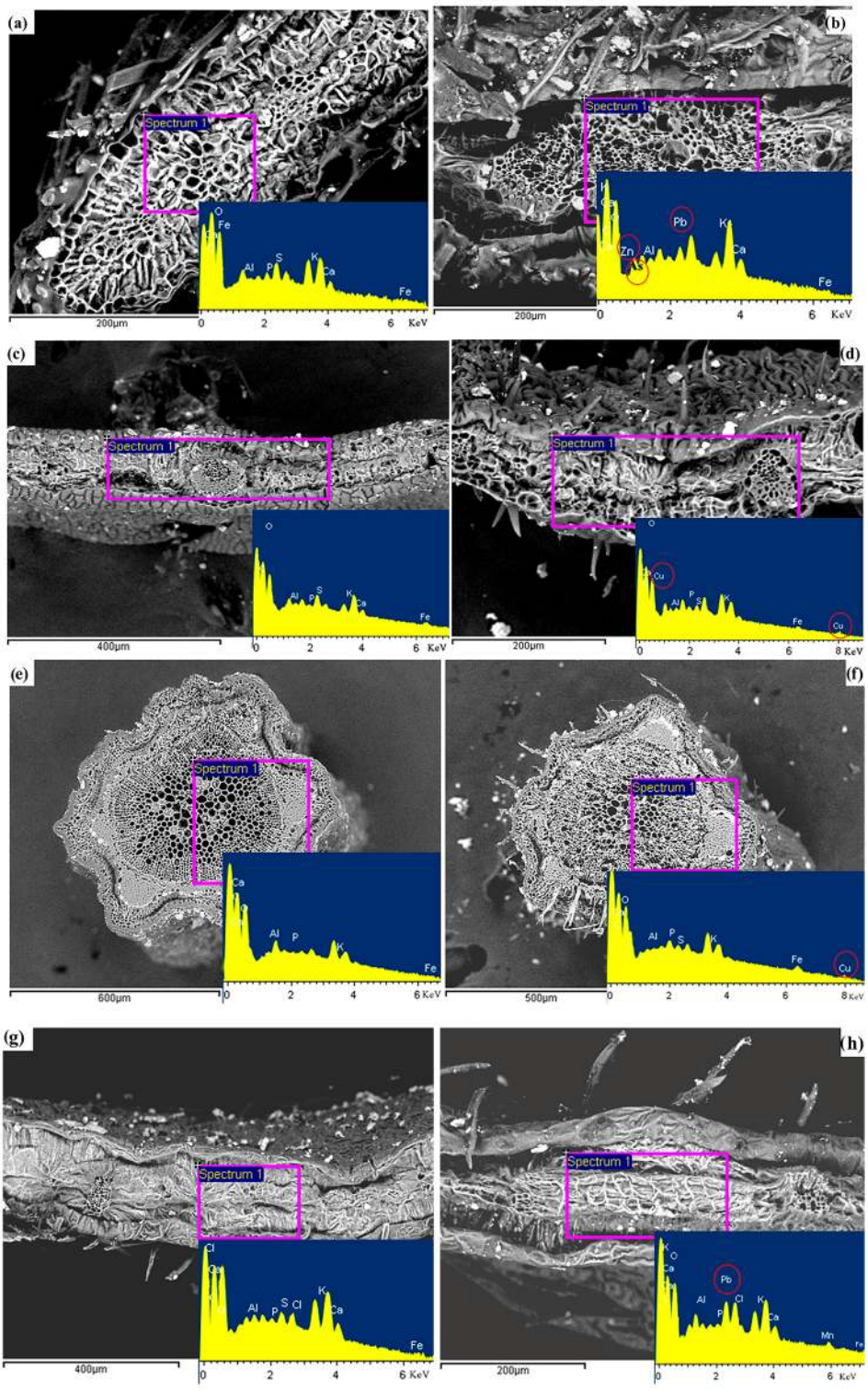

Figure 7. SEM-EDX, elemental mapping of cross sections of aerial organs of *L. cuneifolia*, *B. retama*, and *N. flexuosa*. (**a**,**c**,**g**) correspond to leaves of *L. cuneifolia*, *N. flexuosa*, and *B. retama*, respectively, exposed to T_0. (**e**) corresponds to the stem of *N. flexuosa* exposed to T_0. (**b**,**d**,**h**) leaves of *L. cuneifolia*, *N. flexuosa* and *B. retama*, respectively, exposed to T_{10}. (**f**) stem of *N. flexuosa* exposed to T_{10}. Spectrum: scanning area.

4. Discussion

The increase in the proportion of mining waste in the soil led not only to higher metals(loid) concentrations but also to a decrease in soil pH, as previously documented by Heredia, et al. [29]. In the present study, even low proportions of mining waste of T_1

resulted in notable alterations of soil physicochemical properties. Soil acidification is an intrinsic characteristic of sites contaminated with acid mine drainage. Heredia, et al. [4] reported pH values ranging between 2 and 4. As a consequence, individuals of the four native species exposed to treatments with ≥50% mining waste exhibited 100% mortality within 15 days of exposure. In contrast, the pH of T_0, T_1, and T_{10} exceeded six, which is considered an optimal range for plant development.

Acidic pH not only increases the soluble fraction of metal(loid)s, enhancing their bioavailability through the mineralization and hydrolysis of Fe, Mn, and Al oxides and the release of complexed metal(loid)s [30], but it also inhibits plant growth and development, as the optimal pH range for most plant species lies between 6 and 8 [31,32]. However, in this study, the initial concentration of soluble elements in the T_{50} and T_{100} was comparable to those of the less severe treatments (T_0, T_1 and T_{10}). Despite this similarity, plants only survived in T_0, T_1 and T_{10}, where final average pH was above six. These results indicate that soil acidity was the primary factor driving mortality under high mining waste proportions. Consistently, previous studies have shown that plant survival in mining waste-impacted sites generally occur at pH values above 4.5, whereas the early development of these four native species during germination stage is adversely affected at pH values below 4.9 [4,27].

Across the treatments in which seedlings of the four species under study survived, growth was comparable to or exceeded that of the T_0. Variables such as stem BD and height showed no differences relative to the control, suggesting that the assessed growth parameters possess limited sensitivity to the maximum metal(loid) concentrations tested (1572.6 mg kg^{-1} of As, 25.6 mg kg^{-1} of Cu, 33.0 mg kg^{-1} of Cd, and 742.6 mg kg^{-1} of Zn) over the 90-day exposure period. In contrast, roots, aerial shoot dry biomass production and the number of green leaves were adversely affected under T_{10}, with significant reductions observed in all four species. Previous research conducted on soils from La Planta town reported high toxicity in *Lactuca sativa* L., showing growth inhibition at soil contamination levels below 7.5% [20]. These findings indicate that the native species evaluated in this study are more tolerant than standard bioindicator models such as lettuce, which also tends to accumulate higher metal(loid) concentrations in its leaves.

At the end of the 90 days of chronic exposure, the four species showed high concentrations of metal(loid)s in both roots and aerial organs. Zn concentrations reached 1895.1 mg kg^{-1} in the roots of *P. tetracantha* and 1496.0 mg kg^{-1} in the aerial organs of *L. cuneifolia*. As accumulated up to 2223.2 mg kg^{-1} in the roots of *B. retama* and 676.0 mg kg^{-1} in the aerial organs of *N. flexuosa*. Notably, individuals exhibiting higher Zn accumulation and translocation tended to show reduced Cd translocation and accumulation. This pattern was evident in *L. cuneifolia*, which did not exhibit detectable Cd concentrations in aerial organs under any treatment. Conversely, the opposite trend occurred in *N. flexuosa* under T_{10}, where higher Cd concentrations were detected in aerial tissues. This phenomenon has been previously documented in field studies conducted with the same species [4] and likely reflects shared uptake pathways and transport proteins for Zn and Cd, resulting in competitive absorption and translocation of these elements within the plant [8,33].

These results regarding metal concentration in different vegetative organs are consistent with patterns reported for other known phytoremediating species. For example, *Brassica juncea* (L.) Czern. has been described as a bioaccumulator of Cu, Zn, and Pb, while *Jatropha curcas* L. can accumulate Cu, As, and Zn, with recorded concentrations of 80, 18, and 500 mg kg^{-1}, respectively [34]. The four species evaluated in this work, after 90 days of exposure, presented higher BAF and TF values for Zn, Cd, and As, further confirming their bioaccumulation capacity and phytoremediation potential, in agreement with previous studies [34].

Although the highest Cu concentration was recorded in the roots of *N. flexuosa*, SEM-EDX analysis also detected this element in the leaf and stem tissues. A similar pattern was observed for Cd in *L. cuneifolia*, which, despite its lower concentration in aerial organs, was detected in leaf tissues along with Zn, accumulated at higher concentrations in the shoots. Although Pb was not the primary focus of this study because its soil concentration was below the guideline values established by Law 24,051 for residential and agricultural uses [20], it was detected in the mesophyll of *L. cuneifolia* and *B. retama*. Despite the high concentrations of metal(loid)s detected in the vegetative organs of the four species, no clear histological alterations were observed. This suggests that the toxic elements are not concentrated in a single tissue but are likely distributed or sequestered in different compartments [35].

The Spearman correlation analysis provided further insights into the interactions between plant morpho-physiological responses and metal(loid)s dynamics in the soil. A strong negative correlation was observed between certain metal(loid)s (e.g., As and Zn) and morphological variables such as stem height and number of green leaves, indicating that higher soil metal(loid) concentrations are associated with reduced plant growth. Conversely, positive correlations were found between BAF indices and damage indicators, such as the number of chlorotic and necrotic leaves, suggesting that increased metal(loid) uptake is linked to phytotoxicity symptoms in aerial organs. Furthermore, the significant positive correlations between metal(loid) bioaccumulation in plant organs and the decrease in metals(loid)s in the soil where native seedlings were growing underscore the role of these species in actively removing contaminants from the rhizosphere. This reinforces their potential for in situ phytoremediation strategies.

Increases in APX and POX activity were observed in all four species after 15 days of exposure under T1 compared to T_0. To prevent or reduce damage caused by ROS, plants activate their antioxidant defense system by increasing the activity or production of these enzymes. In many cases, however, the magnitude of the stress can exceed the system's capacity, rendering it insufficient to prevent cellular damage [36]. The high concentrations of metal(loid)s in T_{10}, enhanced MDA production, indicating an insufficient antioxidant response to counteract elevated ROS levels, which leads a state of cellular redox imbalance [37]. This response correlates with severe leaf symptoms of damaged and lower biomass production observed at the end of the exposure period in T_{10}. Under these conditions, normal cellular function is compromised because toxic elements have a high affinity for sulfhydryl and carboxyl groups, thereby disrupting enzymatic and proteins activity [1]. Similar results have been reported in other studies, where metal(loid) exposure reduced antioxidant responses, leading to lower root biomass production, and leaf chlorosis [38,39]. During germination assays, *N. flexuosa* seed antioxidant activity decreased at concentrations above 1500 mg kg^{-1} of As and Zn and 20 mg kg^{-1} of Cu and Cd [29].

Finally, soil microorganisms play a fundamental role in phytoremediation process, contributing to its overall effectiveness. The diversity, abundance, and activity of microbial communities are affected by high concentrations of toxic elements and other soil characteristics such as pH [40]. However, it has been reported that indigenous soil microbiota can increase plant tolerance when exposed to metal(loid)s over extended periods [41]. In the present study, initial microbial abundance was lower in T_{50} and T_{100}, likely due to the combination of higher metal(loid) concentrations and acidic soil pH, which negatively affect microbial growth and survival [31]. Conversely, at the end of the exposure period, yeast and bacterial colonies were more abundant not only in the reference soil (T_0) but also in T_1 and T_{10}. This increase could be attributed to the presence of plant roots, which facilitate the creation of microenvironments conducive to the survival and development

of various microbial communities [42]. A higher number of microorganism colonies may enhance the phytoremediation process, as these communities are essential for maintaining soil productivity [43]. Moreover, microorganisms can participate in metal(loid) sequestration or even accumulate these elements, contributing to the phytostabilization process and preventing the further dispersion of contaminants [44]. Therefore, understanding the interactions between plants and soil microbiota is crucial for optimizing phytoremediation strategies in contaminated environments.

5. Conclusions

The results obtained in this study demonstrate that plant exposure to contamination levels exceeding 10% resulted in 100% mortality in all four selected species within 15 days. Despite this, the species successfully survived and grew in soils with concentrations of As, Cu, Cd, and Zn exceeding those naturally present in the rhizosphere soil of the contaminated site at La Planta, where they currently grow. All four species accumulated metal(loid)s well above levels considered toxic for most plants' development, confirming their bioaccumulation capacity, and tolerance to highly contaminated soils, even within the most severe categories of contamination. The combined use of these native species in a phytoremediation program is particularly relevant, as each species exhibits distinct bioaccumulation and absorption profiles for specific heavy metal(loid)s, thereby enhancing the overall efficiency of multi-element remediation strategies.

The antioxidant response evaluated after 15 days of exposure indicates that at T_{10}, enzymatic activity decreased while MDA levels increased. These biochemical changes may signal long term physiological stress and potential mortality. This response, together with physicochemical factors such as the low pH and high EC present from T_{50} onwards, highlights the need to evaluate different alternatives, such as the application of soil amendments, to facilitate plant establishment under extreme conditions, supporting effective in situ phytoremediation strategies.

Overall, this study provides valuable evidence regarding the combined use of four native species for soil recovery processes. The selection of native species will not only promote plant establishment but also contribute to the restoration of fragile arid ecosystems and the ecosystem services they provide. Further research is needed to improve the survival of native species in soils with over 50% mining waste, particularly through soil properties that may enhance plant establishment and long-term performance.

Supplementary Materials: The following supporting information can be downloaded at https://www.mdpi.com/article/10.3390/environments13030131/s1, Figure S1: Greenhouse conditions: Mean daily temperature during the chronic exposure test in the greenhouse (90 d); Table S1: CF: Contamination Factor (CF) per metal(loid) for each treatment, and the Degree of Contamination (C_{deg}); Table S2: Metal(loid)s in soil: Mean values (± SE) of total and soluble metal(loid) concentration, pH, and EC at the end of the exposure period. Different letters indicate statistical differences between treatments for each specie ($p < 0.05$); Table S3: Toxicological endpoints evaluated at different exposure times during the chronic assay; Table S4: SEM-EDX: Principal elements identified through EDX analysis in the vegetative organs of the studied species.

Author Contributions: Conceptualization, B.H., B.J.Y., M.I.M. and G.R.; methodology, B.H., B.J.Y., M.I.M. and G.R.; formal analysis, B.H.; investigation, B.H., B.J.Y., M.I.M., H.P.B., P.P. and G.R.; resources, G.R.; data curation, B.H.; writing—original draft preparation, B.H.; writing—review and editing, B.J.Y., M.I.M. and G.R.; visualization, B.H.; supervision, G.R.; project administration, G.R.; funding acquisition, G.R. and B.J.Y. All authors have read and agreed to the published version of the manuscript.

Funding: This research was funded by European Union's Horizon 2020 Research and Innovation Program under Grant agreement no. 101006912. Instituto Nacional de Tecnología Agropecuaria (2023-PD-L03-I096, 2023-PE-L02-I003 and 2023-PD-L04-I122), Secretaría de Ciencia, Tecnología e Innovación del Gobierno de San Juan (IDeA-2018-ODS) and Ministerio de Ciencia, Tecnología e Innovación Productiva de Argentina (ANPCyT, PICT-2021-I-INVI-0436).

Data Availability Statement: The original contributions presented in this study are included in the article/Supplementary Materials. Further inquiries can be directed to the corresponding author.

Acknowledgments: The authors acknowledge financial support from the Horizon 2020 Phy2Climate Project, Instituto Nacional de Tecnología Agropecuaria, Secretaría de Ciencia, Tecnología e Innovación del Gobierno de San Juan, and Ministerio de Ciencia, Tecnología e Innovación Productiva de Argentina. Belén Heredia thanks the Consejo Nacional de Investigaciones Científicas y Técnicas for granting her postdoctoral fellowship.

Conflicts of Interest: The authors declare that they have no known competing financial interests or personal relationships that could have appeared to influence the work reported in this paper.

Abbreviations

The following abbreviations are used in this manuscript:

BAF	Bioaccumulation Factor
TF	Translocation Factor
APX	Ascorbate Peroxidase
POX	Guaiacol Peroxidase
MDA	Malondialdehyde
ROS	Reactive Oxygen Species
H_2O_2	Hydrogen Peroxide
TBA	Thiobarbituric Acid
TCA	Trichloroacetic Acid
CFUs	Colony-Forming Units
CF	Contamination Factor
C_{deg}	Contamination Degree
S1	Contaminated Site
S2	Reference Site
T_0	0% Mining Waste
T_1	1% Mining Waste
T_{10}	10% Mining Waste
T_{50}	50% Mining Waste
T_{100}	100% Mining Waste
SEM-EDX	Scanning Electron Microscope and Energy Dispersive X-ray Detector

References

1. Zulfiqar, U.; Farooq, M.; Hussain, S.; Maqsood, M.; Hussain, M.; Ishfaq, M.; Ahmad, M.; Anjum, M.Z. Lead toxicity in plants: Impacts and remediation. *J. Environ. Manag.* **2019**, *250*, 109557. [CrossRef]
2. Sarker, R.K.; Chakraborty, P.; Paul, P.; Chatterjee, A.; Tribedi, P. Degradation of low-density poly ethylene (LDPE) by Enterobacter cloacae AKS7: A potential step towards sustainable environmental remediation. *Arch. Microbiol.* **2020**, *202*, 2117–2125. [CrossRef]
3. Tamma, A.A.; Lejcuś, K.; Fiałkiewicz, W.; Marczak, D. Advancing Phytoremediation: A Review of Soil Amendments for Heavy Metal Contamination Management. *Sustainability* **2025**, *17*, 5688. [CrossRef]
4. Heredia, B.; Tapia, R.; Young, B.J.; Hasuoka, P.; Pacheco, P.; Roqueiro, G. Phytoextraction of Cu, Cd, Zn and As in four shrubs and trees growing on soil contaminated with mining waste. *Chemosphere* **2022**, *308*, 136146. [CrossRef]
5. Okereafor, U.; Makhatha, M.; Mekuto, L.; Uche-Okereafor, N.; Sebola, T.; Mavumengwana, V. Toxic Metal Implications on Agricultural Soils, Plants, Animals, Aquatic life and Human Health. *Int. J. Environ. Res. Public Health* **2020**, *17*, 2204. [CrossRef]
6. Hasan, M.M.; Uddin, M.N.; Ara-Sharmeen, I.; F. Alharby, H.; Alzahrani, Y.; Hakeem, K.R.; Zhang, L. Assisting Phytoremediation of Heavy Metals Using Chemical Amendments. *Plants* **2019**, *8*, 295. [CrossRef]

7. Yan, A.; Wang, Y.; Tan, S.N.; Mohd Yusof, M.L.; Ghosh, S.; Chen, Z. Phytoremediation: A Promising Approach for Revegetation of Heavy Metal-Polluted Land. *Front. Plant Sci.* **2020**, *11*, 359. [CrossRef]
8. Acharya, A.; Bellaloui, N.; Pilipovic, A.; Perez, E.; Maddox-Mandolini, M.; Fuente, H.D.L. Current Assessment and Future Perspectives on Phytoremediation of Heavy Metals. *Plants* **2025**, *14*, 2847. [CrossRef]
9. Jeyakumar, P.; Debnath, C.; Vijayaraghavan, R.; Muthuraj, M. Trends in bioremediation of heavy metal contaminations. *J. Environ. Eng. Res.* **2023**, *28*, 220631. [CrossRef]
10. Tovar-Sánchez, E.; Cervantes-Ramírez, T.; Castañeda-Bautista, J.; Gómez-Arroyo, S.; Ortiz-Hernández, L.; Sánchez-Salinas, E.; Mussali-Galante, P. Response of *Zea mays* to multimetal contaminated soils: A multibiomarker approach. *Ecotoxicology* **2018**, *27*, 1161–1177. [CrossRef]
11. Yadav, P.; Jha, S.; Kumari, P.; Sharma, A.; Singh, S. Exogenous salicylic acid application alleviates chromium toxicity in seedlings of Pea (*Pisum sativum* L.) by reducing chromium uptake and enhancing antioxidative capacity. *Int. J. Phytoremediat.* **2025**, *27*, 1–17. [CrossRef]
12. Roqueiro, G.; Maldonado, S.; Ríos, M.d.C.; Maroder, H. Fluctuation of oxidative stress indicators in *Salix nigra* seeds during priming. *J. Exp. Bot.* **2012**, *63*, 3631–3642. [CrossRef]
13. Liu, Y.; Zhao, H.; Yin, K.; Guo, M.; Wang, Y.; Wang, D.; Zong, H.; Xing, M.J.A. The protective effect of Zn^{2+} on As^{3+} toxicity in common carp: Resistance to oxidative stress, inhibition of endoplasmic reticulum stress, apoptosis and autophagy. *Aquaculture* **2022**, *546*, 737375. [CrossRef]
14. Yan, D.M.; Guo, Z.H.; Huang, F.L.; Ran, H.Z.; Zhang, L. Effect of Calcium Magnesium Phosphate on Remediation Paddy Soil Contaminated with Cadmium Using Lime and Sepiolite. *Huan Jing Ke Xue* **2020**, *41*, 1491–1497. [CrossRef]
15. Mansoor, S.; Ali, A.; Kour, N.; Bornhorst, J.; AlHarbi, K.; Rinklebe, J.; Abd El Moneim, D.; Ahmad, P.; Chung, Y.S.J.P. Heavy metal induced oxidative stress mitigation and ROS scavenging in plants. *Plants* **2023**, *12*, 3003. [CrossRef]
16. Yang, J.; Huang, Y.; Zhao, G.; Li, B.; Qin, X.; Xu, J.; Li, X.J.C. Phytoremediation potential evaluation of three rhubarb species and comparative analysis of their rhizosphere characteristics in a Cd-and Pb-contaminated soil. *Chemosphere* **2022**, *296*, 134045. [CrossRef]
17. Feki, K.; Tounsi, S.; Mrabet, M.; Mhadhbi, H.; Brini, F. Recent advances in physiological and molecular mechanisms of heavy metal accumulation in plants. *Environ. Sci. Pollut. Res.* **2021**, *28*, 64967–64986. [CrossRef]
18. Bian, F.; Zhong, Z.; Li, C.; Zhang, X.; Gu, L.; Huang, Z.; Gai, X.; Huang, Z. Intercropping improves heavy metal phytoremediation efficiency through changing properties of rhizosphere soil in bamboo plantation. *J. Hazard. Mater.* **2021**, *416*, 125898. [CrossRef]
19. Tiodar, E.D.; Văcar, C.L.; Podar, D. Phytoremediation and Microorganisms-Assisted Phytoremediation of Mercury-Contaminated Soils: Challenges and Perspectives. *Int. J. Environ. Res. Public Health* **2021**, *18*, 2435. [CrossRef]
20. Calabró, M.R.; Roqueiro, G.; Tapia, R.; Crespo, D.C.; Bargiela, M.F.; Young, B.J. Chronic toxicity, bioavailability and bioaccumulation of Zn, Cu and Pb in Lactuca sativa exposed to waste from an abandoned gold mine. *Chemosphere* **2022**, *307*, 135855. [CrossRef]
21. Villagra, P.E.; Passera, C.B.; Greco, S.; Sartor, C.E.; Meglioli, P.A.; Alvarez, J.A.; Dágata, S.; Vega Riveros, C.; Allegretti, L.I.; Fernández, M.E. Ecological restoration and productive recovery of saline environments from the Argentine Monte Desert using native plants. In *Saline and Alkaline Soils in Latin America: Natural Resources, Management and Productive Alternatives*; Springer International Publishing: Cham, Switzerland, 2021; pp. 313–338.
22. USEPA. *U.E.P.A. Standard Elutriate Preparation. Guidance for performing Tier II Evaluations. Evaluation of Dredged Material Proposed for Discharge in Waters of the U.S.—Testing Manual*; USEPA: Washington, DC, USA, 1998.
23. Hakanson, L. An ecological risk index for aquatic pollution control.a sedimentological approach. *Water Res.* **1980**, *14*, 975–1001. [CrossRef]
24. Poschenrieder, C.; Bech, J.; Llugany, M.; Pace, A.; Fenés, E.; Barceló, J. Copper in plant species in a copper gradient in Catalonia (North East Spain) and their potential for phytoremediation. *Plant Soil* **2001**, *230*, 247–256. [CrossRef]
25. Xu, T.; Xie, F.; Wei, Z.; Zeng, S.; Wu, Q.T. Phytoremediation of sewage sludge and use of its leachate for crop production. *Environ. Technol.* **2015**, *36*, 3000–3007. [CrossRef]
26. Bradford, M.M. A rapid and sensitive method for the quantitation of microgram quantities of protein utilizing the principle of protein-dye binding. *Anal. Biochem.* **1976**, *72*, 248–254. [CrossRef]
27. Heath, R.L.; Packer, L. Photoperoxidation in isolated chloroplasts: I. Kinetics and stoichiometry of fatty acid peroxidation. *Arch. Biochem. Biophys.* **1968**, *125*, 189–198. [CrossRef] [PubMed]
28. Kurtzman, C.P. Three new ascomycetous yeasts from insect-associated arboreal habitats. *Can. J. Microbiol.* **1999**, *46*, 50–58. [CrossRef]
29. Heredia, B.; Recio, P.D.; Young, B.J.; Pacheco, P.; Zungre, F.B.; Hruby, S.; Acevedo, M.A.; Mercado, M.I.; Roqueiro, G. Strategies of physiological, morpho-anatomical and biochemical adaptation in seedlings of native species exposed to mining waste. *Ecotoxicol. Environ. Saf.* **2025**, *290*, 117750. [CrossRef]

30. Kicińska, A.; Pomykała, R.; Izquierdo-Diaz, M. Changes in soil pH and mobility of heavy metals in contaminated soils. *Eur. J. Soil Sci.* **2022**, *73*, e13203. [CrossRef]
31. Wang, C.; Wu, B.; Jiang, K.; Wei, M.; Wang, S. Effects of different concentrations and types of Cu and Pb on soil N-fixing bacterial communities in the wheat rhizosphere. *Appl. Soil Ecol.* **2019**, *144*, 51–59. [CrossRef]
32. Li, X.; Cao, Y.; Xiao, J.; Salam, M.M.A.; Chen, G. Bamboo biochar greater enhanced Cd/Zn accumulation in Salix psammophila under non-flooded soil compared with flooded. *Biochar* **2022**, *4*, 7. [CrossRef]
33. Zhang, B.; Zhang, X.; Luo, L. The major gene families related to cadmium absorption and transportation in plants. *Genom. Appl. Biol.* **2013**, *32*, 127–134. Available online: https://cabidigitallibrary.org/doi/full/10.5555/20133131726 (accessed on 6 February 2026).
34. Cioica, N.; Tudora, C.; Iuga, D.; Deak, G.; Matei, M.; Nagy, E.M.; Gyorgy, Z. A review on phytoremediation as an ecological method for in situ clean up of heavy metals contaminated soils. In *Proceedings of the E3S Web of Conferences*; EDP Sciences: Hulls, France, 2019; p. 03024.
35. Thakur, M.; Praveen, S.; Divte, P.R.; Mitra, R.; Kumar, M.; Gupta, C.K.; Kalidindi, U.; Bansal, R.; Roy, S.; Anand, A.; et al. Metal tolerance in plants: Molecular and physicochemical interface determines the "not so heavy effect" of heavy metals. *Chemosphere* **2022**, *287*, 131957. [CrossRef]
36. Phua, S.Y.; De Smet, B.; Remacle, C.; Chan, K.X.; Van Breusegem, F. Reactive oxygen species and organellar signaling. *J. Exp. Bot.* **2021**, *72*, 5807–5824. [CrossRef]
37. Xie, X.; He, Z.; Chen, N.; Tang, Z.; Wang, Q.; Cai, Y. The Roles of Environmental Factors in Regulation of Oxidative Stress in Plant. *BioMed Res. Int.* **2019**, *2019*, 9732325. [CrossRef]
38. Namdjoyan, S.; Namdjoyan, S.; Kermanian, H. Phytochelatin synthesis and responses of antioxidants during arsenic stress in Nasturtium officinale. *Russ. J. Plant Physiol.* **2016**, *63*, 739–748. [CrossRef]
39. Ahmad, A.; Khan, W.U.; Shah, A.A.; Yasin, N.A.; Naz, S.; Ali, A.; Tahir, A.; Batool, A.I. Synergistic effects of nitric oxide and silicon on promoting plant growth, oxidative stress tolerance and reduction of arsenic uptake in Brassica juncea. *Chemosphere* **2021**, *262*, 128384. [CrossRef]
40. Sharma, P.; Dutta, D.; Udayan, A.; Nadda, A.K.; Lam, S.S.; Kumar, S. Role of microbes in bioaccumulation of heavy metals in municipal solid waste: Impacts on plant and human being. *Environ. Pollut.* **2022**, *305*, 119248. [CrossRef] [PubMed]
41. Al Mahmud, J.; Bhuyan, M.B.; Anee, T.I.; Nahar, K.; Fujita, M.; Hasanuzzaman, M. Reactive oxygen species metabolism and antioxidant defense in plants under metal/metalloid stress. In *Plant Abiotic Stress Tolerance: Agronomic, Molecular and Biotechnological Approaches*; Springer International Publishing: Cham, Switzerland, 2019; pp. 221–257.
42. Hu, J.; Yang, T.; Friman, V.-P.; Kowalchuk, G.A.; Hautier, Y.; Li, M.; Wei, Z.; Xu, Y.; Shen, Q.; Jousset, A. Introduction of probiotic bacterial consortia promotes plant growth via impacts on the resident rhizosphere microbiome. *Proc. R. Soc. B* **2021**, *288*, 20211396. [CrossRef]
43. Zhao, R.; Cao, X.; Li, X.; Li, T.; Zhang, H.; Cui, X.; Cui, Z. Ecological toxicity of Cd, Pb, Zn, Hg and regulation mechanism in *Solanum nigrum* L. *Chemosphere* **2023**, *313*, 137447. [CrossRef]
44. Sarker, A.; Al Masud, M.A.; Deepo, D.M.; Das, K.; Nandi, R.; Ansary, M.W.R.; Islam, A.R.M.T.; Islam, T. Biological and green remediation of heavy metal contaminated water and soils: A state-of-the-art review. *Chemosphere* **2023**, *332*, 138861. [CrossRef] [PubMed]